Geophys. J. R. astr. Soc. (1985) **81**, 89–101

Anisotropic propagation of *P*- and *S*-waves in the western Pacific lithosphere

Rhett Butler *Hawaii Institute of Geophysics, University of Hawaii, 2525 Correa Road, Honolulu, Hawaii 96822, USA*

Accepted 1984 September 17. Received 1984 September 12; in original form 1984 June 12

Summary. Apparent velocities for oceanic *P* and *S* phases from NW circum-Pacific earthquakes recorded on an ocean bottom hydrophone array near Wake Island vary with azimuth of approach. The apparent velocity data from events in the Mariana Islands are fast, whereas velocities of events between the Izu-Bonin Islands and the Kurils are slower. For data showing slow apparent velocities, the path average group velocity exceeds the local apparent velocity. The azimuthal variation of oceanic *P* and *S* apparent velocity is consistent with azimuthal anisotropy, and the slow direction of propagation is nearly parallel to the strike of local magnetic lineations. Propagation paths that parallel the local magnetic lineations near the OBH array are more perpendicular to lineations in the region of the NW Pacific basin where the paths originate. The observation of path group velocity faster than local apparent velocity for oceanic *P* and *S* is qualitatively consistent with a re-orientation of anisotropy as manifested in the magnetic lineations along the propagation path between source and receiver. Results suggest that the western Pacific lithosphere is azimuthally anisotropic for *P*- and *S*-wave propagation.

Introduction

In the western Pacific the dominant seismic phases observed on island stations and ocean bottom seismometers and hydrophones are the long-range, high-frequency (2–30 Hz) *P* and *S* phases that propagate with velocities appropriate for *Pn*/*Sn*. These phases have been discussed in a series of papers by scientists at the Hawaii Institute of Geophysics (e.g. Walker & Sutton 1971; Sutton & Walker 1972; Walker 1977; Sutton *et al.* 1978; Walker *et al.* 1978; McCreery & Sutton 1980; Walker, McCreery & Sutton 1983). Although these phases have been commonly called *Pn*/*Sn*, their great propagation distances (> 2000 km) and frequency contents would indicate that we are dealing with an oceanic lithosphere phase and not a simple head wave implied by the nomenclature '*Pn*/*Sn*'. At HIG these phases have come to be called oceanic *P* and *S* after Walker (1982). This paper presents a re-examination of data from an ocean bottom hydrophone (OBH) array deployment reported by Walker & McCreery (1985). Two indications for azimuthal anisotropic propagation of oceanic P and S in the Western Pacific lithosphere were discovered: (1) azimuthally varying local apparent velocity and (2) path group velocity faster than local apparent velocity. In this paper statistical uncertainties in observation (1) are calculated. Observation (2) is shown to be consistent with an azimuthally varying velocity along the propagation paths of oceanic P and S due to a change in anisotropic alignment, which is also expressed in the changing orientation of local magnetic lineations along the path.

Observations of anisotropy in the Pacific

An isotropic material is characterized by a velocity independent of direction. Anisotropy implies that certain directions are characterized by faster or slower velocities. Anisotropy is usually discussed for two more simple symmetry categories: (1) horizontal wavespeed varying as a function of azimuth of propagation (azimuthal anisotropy); and (2) horizontal wavespeed not equal to vertical wavespeed (transverse or polarization anisotropy).

The existence of anisotropy in the Pacific was first discovered in marine seismic refraction data in the NE Pacific by Hess (1964) who reported a high correlation between mantle velocity and spreading direction. Hess (1964) also suggested that the anisotropy was due to a preferential alignment of olivine crystals, as olivine is both a major constituent of the mantle and significantly anisotropic. Backus (1965) discussed the possible forms of seismic anisotropy and their influence on body waves. Refined multi-ship refraction experiments in several locations between Hawaii and North America established the azimuthal anisotropy of the compressional velocity below the Moho (Raitt *et al.* 1969; Raitt 1969; Morris, Raitt & Shor 1969; Keen & Barrett 1971; Raitt *et al.* 1971). The fast propagation direction lay approximately parallel to the spreading direction at the time of lithosphere formation, parallel to the fracture zones, and perpendicular to the magnetic lineaments. The slow direction was found to be parallel to the magnetic lineaments. The velocity difference between fast and slow directions is 0.6–0.7 km s^{-1} relative to a mean velocity of 8.1–8.2 km s^{-1}. Scrutinizing available Scripps marine refraction data in the Pacific, Bibee & Shor (1976) reported that the sub-Moho compressional velocity showed widespread anisotropy averaging about 5 per cent in magnitude with the fast direction perpendicular to the magnetic anomalies – in agreement with previous results. All of the above studies are generally based upon refraction lines less than 250 km long and, consequently, the anisotropy effects observed represent only the uppermost part of Pacific lithosphere. With few exceptions the observations lie in the eastern Pacific where the lithospheric age is less than 100 Ma. The only apparent exception to the observations that the anisotropic *Pn* fast direction lies perpendicular to the magnetic lineations is in data from French Polynesia. Talandier & Bouchon (1979) reported *Pn* velocity variation of 0.1 km s^{-1} over a 40° azimuthal window from an earthquake north of Gambier Island, and the fast direction lay along the trend of the Tuamotu Archipelago – about 30° clockwise to magnetic lineations.

In the north-western Pacific basin Shimamura & Asada (1983) and Shimamura (1984) have reported evidence for anisotropy in the distance range 140–1800 km. Average velocities of P and S were 8.6 and 4.88 km s^{-1}, respectively, on the N–S line, and 8.05 and 4.53 km s^{-1} on the nearly E–W line. The maximum velocity was nearly perpendicular to the magnetic lineations. Shimamura & Asada further stated that the anisotropy extends to significant depth below Moho in the lithosphere, on the basis of observed offsets in the travel-time curves.

Surface wave studies of the Pacific reveal the existence of polarization anisotropy in the upper 200 km (or so) of the mantle (e.g. Forsyth, 1975a, b; Schlue & Knopoff 1976, 1977, 1978; Yu & Mitchell 1979; Mitchell & Yu 1980; Anderson & Regan 1983). The requirement of polarization anisotropy comes from the inconsistency of Rayleigh and Love waves dispersion data (McEvilly 1964; Anderson 1966). For derivation of a structure consistent with both data sets, the horizontal velocity must be faster than the vertical velocity. Specific models to fit the Rayleigh and Love wave data have been non-unique. Schlue & Knopoff (1976, 1977, 1978) and Anderson & Regan (1983) detected polarization anisotropy in the asthenosphere, but little or no anisotropy in the Pacific lithosphere. Yu & Mitchell (1979) and Mitchell & Yu (1980) resolved polarization anisotropy in the Pacific lithosphere, but not in the asthenosphere. Knopoff (1983) presented some discussion of this apparent dichotomy. Methods and datasets used in the different studies have varied, and we might expect some consensus to be reached in further developments. However, the fundamental mode Love and Rayleigh wave data do not contain sufficient information to resolve, simultaneously and uniquely, anisotropy, lithosphere thickness, and regional variation of velocity structure with lithospheric age.

Very little azimuthal anisotropy has been detected in the surface wave data. Smith & Dahlen (1973) derived the form of the azimuthal dependence of Love and Rayleigh wave phase velocities for a slightly anisotropic medium. Forsyth (1975a, b) found a 2 per cent azimuthal Rayleigh wave (fundamental mode) velocity variation in the Nazca plate, with the maximum velocity locally perpendicular to the magnetic lineations. The Love waves (fundamental mode) showed a similar variation at long periods, but at a lower (90 per cent) level of confidence. The age of the region was less than 50 Ma. In the studies by Schlue & Knopoff (1976, 1977, 1978) of the regionalized Pacific, azimuthal anisotropy of Love and Rayleigh waves was as large as the uncertainties in the data. Yu & Mitchell (1979) and Mitchell & Yu (1980) found that when they assumed a uniform azimuthal anisotropy for the Pacific lithosphere, the Rayleigh and Love data indicated that the fast velocity direction (0.8 per cent) is oriented roughly E–W. A regionalization of the Pacific assuming independently oriented anisotropy in different ages of lithosphere reduced rms time errors in the Love and Rayleigh data by 2 s, but further model calculations were not reported. Surface waves are sensitive primarily to the shear wave velocity. The period range in the above studies is 30–100 + s corresponding to wavelengths of 100–450 + km. Studying the particle motion of short-period surface waves in the Pacific basin, Kirkwood & Crampin (1981) found polarization anomalies consistent with either weak azimuthal anisotropy throughout the lithosphere or strong azimuthal anisotropy throughout the asthenosphere. Forsyth (1975a, b) has noted that although velocity structures with only shear wave (azimuthal) anisotropy leads to well-defined models fitting the Rayleigh wave data, the inclusion of P-wave anisotropy makes the problem highly non-unique.

Ocean bottom hydrophone deployment

Late in the summer of 1981, the Hawaii Institute of Geophysics (HIG) successfully deployed a 1600 km long linear array of 12 ocean bottom hydrophones (OBHs) near Wake Island (Fig. 1). Details of the experiment and preliminary results are presented in Walker & McCreery (1985). Half of the instruments began recording on August 12 and stopped on September 23. The remaining half started on September 3 and finished on October 15. The total recording time was about 65 days, and all 12 instruments were in operation from September 3 to September 23. Of the 12 OBHs deployed, 10 were successfully recovered, and nine of these recorded quality data throughout their period of operation. Recording concurrently were three bottom hydrophones of the Wake Hydrophone Array (WHA), a 40-km aperture array of sensors cabled directly to Wake Island. Data from 10 shallow-focus (< 100 km) earthquakes in the distance range 18–33° were used to compute propagation velocities for oceanic P and S phases. The travel-time and distance data from the 10 events

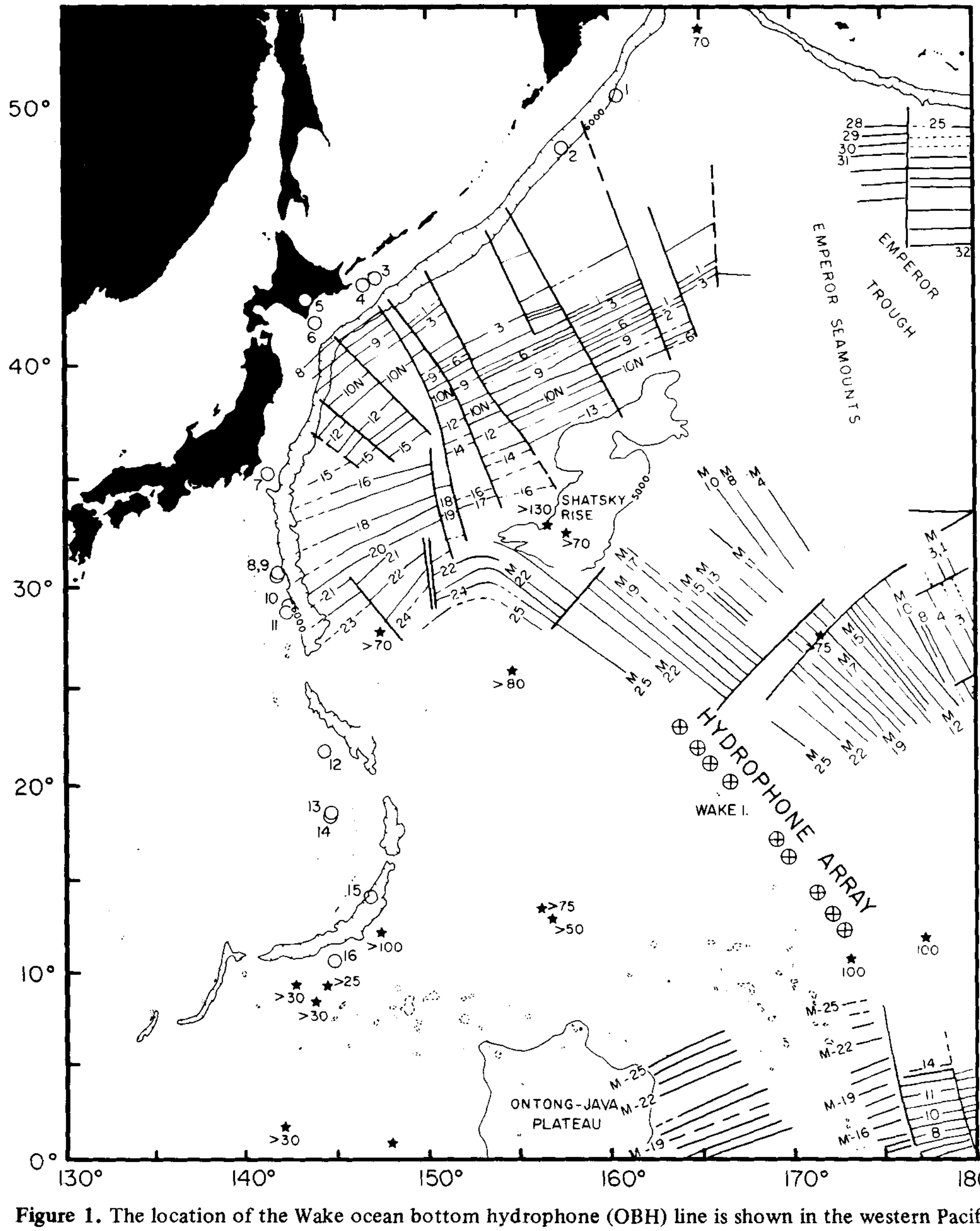

Figure 1. The location of the Wake ocean bottom hydrophone (OBH) line is shown in the western Pacific. OBH locations are plotted as a plus within a circle. Earthquakes are plotted as open circles with numbers indexed to Table 1. Selected DSDP drill sites are noted by stars with minimum ages in millions of years. Magnetic lineations are from Hilde, Isezaki & Wageman (1976) and Larson (1976).

were merged and the best fitting (in a least-squares sense) straight line determined the apparent velocity and intercept.

The resulting travel-time equations of $T = X/(7.96 \pm 0.05\,\mathrm{km\,s^{-1}}) - (7.14 \pm 2.38\,\mathrm{s})$ for P-waves and $T = X/(4.57 \pm 0.04\,\mathrm{km\,s^{-1}}) - (14.03 \pm 5.31\,\mathrm{s})$ for S-waves yielded two surprises, the first being the apparent propagation velocities. *Pn* velocities of about $8.3\,\mathrm{km\,s^{-1}}$ and *Sn* velocities of about $4.8\,\mathrm{km\,s^{-1}}$ were previously reported in the NW Pacific by Walker &

Sutton (1971), Sutton & Walker (1972), and Walker (1977). These previously reported velocities were determined by regression analysis on the times and distances of *Pn* and *Sn* observations from circum-Pacific earthquakes recorded on Pacific island stations (including Wake). It is perhaps not surprising that an array experiment would obtain somewhat different results than a regression analysis of the propagation times of many earthquakes to single island stations; the magnitude of the discrepancy is surprising. For both oceanic *P* and *S* the apparent velocity decrease is about 4 per cent. For oceanic *S* the apparent velocity of 4.57 km s^{-1} is comparable to the *Sn* velocity of 4.58 km s^{-1} that Hart & Press (1973) reported for the regionalized Atlantic of age less than 50 Ma; however, the age of the lithosphere in the area of OBH deployment is about 150 Ma. The second surprising result reported by the Walker & McCreery (1985) study was the negative intercept time, extrapolated to zero distance for both oceanic *P*- and *S*-waves. Earlier studies by Walker & Sutton (1971), Sutton & Walker (1972), and Walker (1977) all reported positive intercepts. The negative intercept indicates that the apparent velocity of the waves propagating across the array is too slow to account for the time and distance required in propagating from the sources to the array, and implies that the waves travelled with a higher velocity somewhere between the source and the array.

Azimuthal propagation effects

Distance ($\Delta°$) and reduced travel time of the oceanic *P* and *S* phases are plotted in Figs 2 and 3 for earthquakes of the NW circum-Pacific recorded during the deployment. Table 1 lists the epicentral data for each event. Eleven events had well-recorded *P*-waves on three or more OBHs, and 10 events yielded well-recorded *S*-waves on each of three or more instruments. To regionalize the data, both with regard to azimuth and epicentral region, the data were divided into three groups.

In Fig. 2 for the *P*-waves we see that there is a considerable range in the slopes of the least-squares lines. In Fig. 3 this range is also evident for the *S*-waves. The data from the

Table 1. Epicentres of NW circum-Pacific earthquakes recorded by HIG hydrophones.

Date	Origin Time	Lat°N	Long°E	Depth (km)	m_b	Region	Index #
8/23/81	12:00:25:6	48.687	157.425	33	6.0	Kurils	2
8/26/81	04:51:37.1	14.095	146.699	46	5.1	Marianas	15
9/03/81	05:35:44.8	43.594	147.079	46	6.6	Kurils	3
9/07/81	19:06:02.6	30.609	141.614	33	5.8	Izu-Bonin	8
9/07/81	20:07:26.0	30.611	141.611	41	5.1	Izu-Bonin	9
9/08/81	19:26:27.6	43.373	146.485	52	5.7	Kurils	4
9/10/81	23:21:24.2	10.671	144.735	15	5.5	South of Marianas	16
9/12/81	14:51:27.2	42.769	143.302	110	4.9	Hokkaido	5
9/14/81	15:08:32.9	29.018	142.285	33	5.4	Izu-Bonin	10
9/24/81	02:40:47.0	41.839	143.834	39	5.3	Hokkaido	6
9/24/81	17:20:49.7	28.968	142.291	33	5.7	Izu-Bonin	11
10/01/81	17:04:44.7	50.677	160.497	33	5.9	Kurils	1
10/02/81	15:13:27.1	21.755	144.343	119	5.0	Marianas	12
10/04/81	04:11:03.5	35.266	141.021	42	5.2	East Coast of Honshu	7
10/14/81	12:29:41.3	18.492	145.653	205	5.0	Marianas	14
10/14/81	20:09:06.2	18.552	145.729	168	5.1	Marianas	13

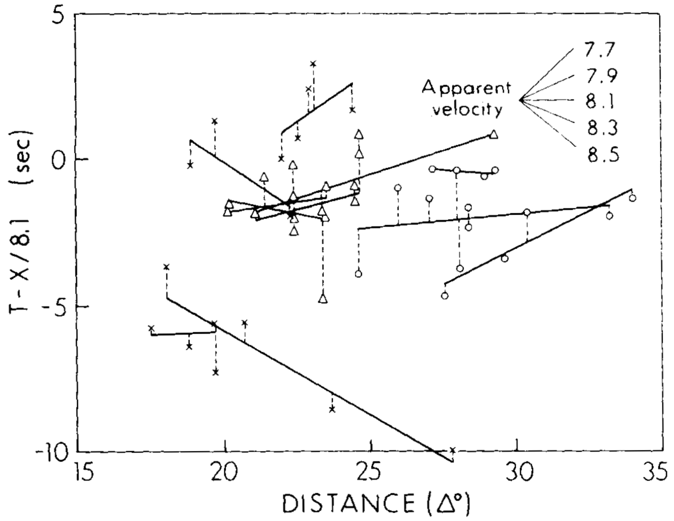

Figure 2. Apparent velocity (km s^{-1}) for oceanic *P*-waves are determined from a least-square fit to earthquake data. Three epicentral regions are plotted: crosses for Marianas, triangles for Izu-Bonin to Japan, and circles for Kuril earthquakes. A substantial variation of apparent velocity may be observed.

Marianas in Figs 2 and 3 exhibit apparent velocities faster than the reducing velocity (8.1 km s^{-1} for *P* and 4.65 km s^{-1} for *S*). For the Japan–Izu–Bonin data and the Kurils data the apparent velocities are slower than the reducing velocities.

The data in Figs 2 and 3 do not show a systematic distance effect. The apparently faster Marianas data are closer than the Japanese and Kurils data, but some of the slowest events are at intermediate distances. All of these data represent the high-frequency, oceanic *P* and *S* phases, and are not the first arriving, mantle-refracted *P*- and *S*-waves. All of the times were hand-picked independently by two observers.

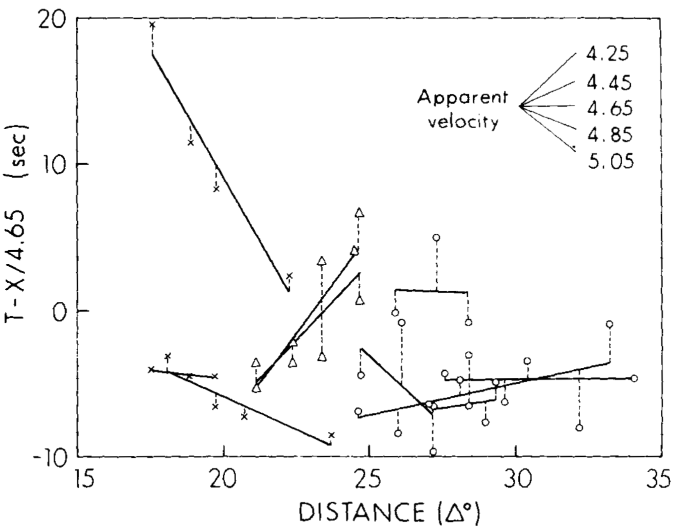

Figure 3. Apparent velocity (km s^{-1}) for oceanic *S*-waves are determined from a least-square fit to earthquake data. Three epicentral regions are plotted: crosses for Marianas, triangles for Izu-Bonin to Japan, and circles for Kuril earthquakes. A substantial variation of apparent velocity may be observed.

Apparent velocity data reduction

Apparent velocities of the oceanic *P*- and *S*-waves may be derived immediately from the inverse slopes of the least-squares lines in Figs 2 and 3. However, to obtain a better feel for the statistical significance of these data, Student's *t*-distribution is used to estimate 95 per cent confidence limits on the regression slopes. The data are then smoothed by averaging apparent velocity data from earthquakes in the same azimuth window by the maximum likelihood method.

The sum of squares of deviations, $\Sigma d_{y \cdot x}^2$, is the basis for an estimate of error in fitting the line $T = aX + b$ (Snedecor & Cochran 1967). The mean square deviation from regression is

$$S_{y \cdot x}^2 = \Sigma d_{y \cdot x}^2 / (n-2) \tag{1}$$

where $(n-2)$ is the number of degrees of freedom. The sample standard deviation of the regression coefficient is

$$S_a = \sqrt{S_{y \cdot x}^2 / x^2} \tag{2}$$

where $x^2 = \Sigma(X - \bar{X})^2$ and X is the distance and $\bar{X}$ is the mean distance. The population regression coefficient α_i for event i has 95 per cent confidence limits calculated from the sample regression coefficient

$$a - t_{0.05} S_a < \alpha_i < a + t_{0.05} S_a \tag{3}$$

where $t_{0.05}$ is the value from the *t*-distribution with $(n-2)$ degree of freedom. The range of apparent velocity V at a 95 per cent level of confidence is the inverse slope of

$$v_i = 1/\alpha_i \tag{4}$$

and the uncertainty of α_i is determined by relation (3).

For each event we now have a means to estimate the 95 per cent confidence interval for the apparent velocity derived from the regression analysis. When averaging data with uncertainties, it is best to lend more weight to the data with smaller uncertainty. In the maximum likelihood method of averaging data, the data are weighted by the reciprocals of the sample variances, $1/S_a^2$. For data with 95 per cent confidence limits calculated by the *t*-distribution, we can use the reciprocal of the squares of the 95 per cent confidence limits, $1/(t_{0.05} S_a)^2$. The maximum likelihood value of the inverse apparent velocity is

$$\alpha = \frac{\Sigma_i a_i / e_i^2}{\Sigma_i 1/e_i^2} \tag{5}$$

where a_i is the regression coefficient (slope) from the ith event and $e_i = (t_{0.05} S_a)_i$ = 95 per cent confidence limit of a_i. The averaged (squared) uncertainty of α is

$$\frac{1}{e^2} = \Sigma_i (1/e_i^2) \tag{6}$$

and thus the apparent velocity V lies between

$$1/(\alpha + e) < V < 1/(\alpha - e) \tag{7}$$

at a 95 per cent level of confidence.

Figs 4 and 5 present the data of Figs 2 and 3 as a polar plot of azimuth of approach to the Wake line experiment and apparent velocity. Velocity increases radially and azimuth is

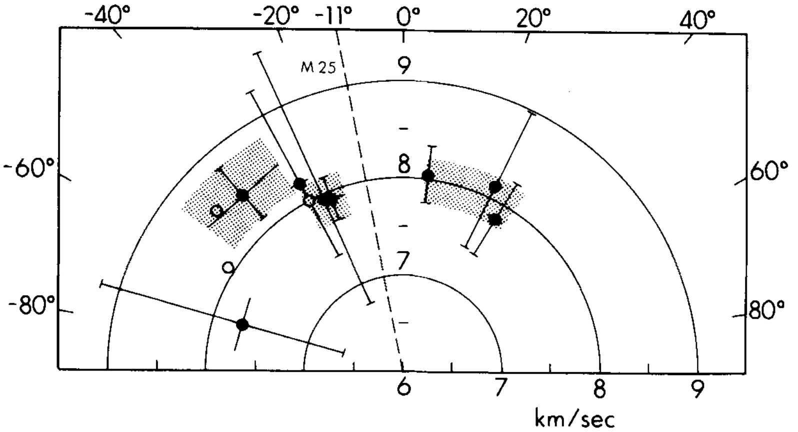

Figure 4. A polar plot of apparent velocity versus azimuth of approach (relative to 322°, the NW trend of the array) for oceanic *P* data. Apparent velocity increases radially outward. Error bounds on velocity are 95 per cent confidence intervals. Data plotted as open circles have error bounds too large to be plotted on figure. Azimuth error bounds plot azimuth windows subtended between array elements closest to and furthest from the events. Shaded regions present maximum likelihood averages of apparent velocity in each of three regions. Dashed line at −11° shows relative strike of nearby Mesozoic magnetic lineament M25, which has an age of about 150 Ma.

measured from the strike of the linear array (positive is clockwise from the array pointing NW). The 95 per cent confidence limits are given for each well-constrained apparent velocity. Each datum is plotted azimuthally with respect to the strike of the array, and azimuthal error bounds give the spread of azimuth observed between OBH sites closest and furthest from the event. Open circles represent events whose uncertainty of slope is off the scale of the figure (i.e. lines with few stations and lines with short length are more uncertain). Events are grouped into the three regions discussed earlier, and the apparent velocities in

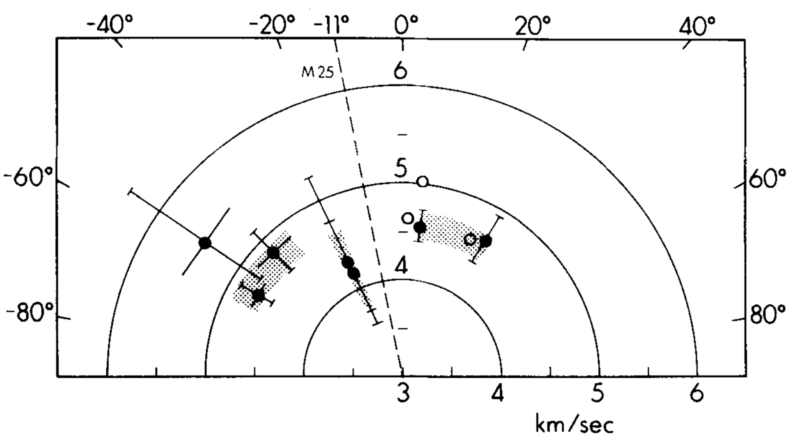

Figure 5. A polar plot of apparent velocity versus azimuth of approach (relative to 322°, the NW trend of the array) for oceanic *S* data. Apparent velocity increases radially outward. Error bounds on velocity are 95 per cent confidence intervals. Data plotted as open circles have error bounds too large to be plotted on figure. Azimuth error bounds plot azimuth windows subtended between array elements closest to and furthest from the events. Shaded regions present maximum likelihood averages of apparent velocity in each of three regions. Dashed line at −11° shows relative strike of nearby Mesozoic magnetic lineament M25, which has an age of about 150 Ma.

each group are averaged. The shaded areas are bounded by the azimuthal windows and 95 per cent confidence intervals of apparent velocity for the three regions. For the Marianas group the two events at the far left of Fig. 4 contribute very little to the average, and consequently are not included in the shading.

The oceanic *P* and *S* polar plots (Figs 4 and 5, respectively) have the same format. The dashed line at counter-clockwise 11° is the strike of local magnetic anomaly M25, which is dated at about 150 Ma. The apparent velocity data closest to this strike are the slowest. The data from Izu-Bonin through Japan and the Kurils are typically slower than the better apparent velocity measurements from the Marianas. The slow region lies within a 30° angle from the trend of the array, which includes the local azimuth of the nearby Mesozoic magnetic anomalies. The region of the array itself lies in a magnetic quiet zone.

At a 95 per cent level of confidence, these three areas are not mutually exclusive. At a 94 per cent level, however, the Marianas *P*- and *S*-wave data are faster than the more northerly events. Thus the pattern of apparent velocity variation which was observed in Figs 2 and 3 may be viewed in the context of azimuth of approach. Naturally, the Wake OBH line experiment was not designed to capture azimuthal effects best. The data from the Marianas have a wide azimuth window between closest and furthest array elements, with the closer elements having greater angles with the array. With the OBH sites further from the Marianas events at shallower angles to the trend of the array, these further data may experience slower apparent velocities, if the velocity is azimuthally dependent. In fact, if the apparent velocity of the Marianas events are recomputed without the farthest OBH sites, the apparent velocity increases for the set of near stations with propagation at steeper angles to the array.

The low composite values of 7.96 km s^{-1} for *P*-waves and 4.57 km s^{-1} for *S*-waves found by Walker & McCreery (1985) represent averages over azimuthal variations, weighted toward the azimuths of Japan and the Kurils due to the larger number of events.

Discussion

The apparent velocity data provided in Figs 2–5 lend circumstantial evidence for azimuthal anisotropic propagation of *P*- and *S*-waves in the western Pacific basin. The data cannot uniquely constrain the anisotropy, and the azimuthal variation is not robust at a 95 per cent level of confidence. The evidence for azimuthally varying velocity, however, coupled with the negative time intercepts for least-squares regression lines, strongly suggests either azimuthal velocity anisotropy or regionally varying velocity. Although regional velocity variations cannot be dismissed, the existence of azimuthal velocity anisotropy in the lithosphere correlated with the magnetic lineations lends a simple explanation to the negative intercept problem.

The slow apparent velocities for the Japanese and Kuril data which travel more along the strike of the OBH line have group arrival times indicating faster velocities for the whole path than for the local apparent velocity across the array. As Walker & McCreery (1985) pointed out, this indicates that the *P* and *S* velocities must be faster along some part of the propagation path. The work of Raitt *et al.* (1969), Morris *et al.* (1969), Keen & Barrett (1971), and Bibee & Shore (1976) shows that the compressional velocity of the sub-Moho mantle tends toward a minimum along the strike of the local magnetic lineations. This velocity minimum usually lies within 17° of the strike of magnetic stripes, with the fast direction perpendicular. The azimuthal velocity distribution depends upon the anisotropy. An azimuthal dependence of $\cos 2\theta$ and, more rarely, $\cos 4\theta$ are observed for compressional waves. The OBH line experiment of Fig. 1 lies in a magnetic quiet zone, but nearby magnetic lineations strike about 11° counter-clockwise from the line of the array (see Figs 4 and 5).

Therefore, the slow velocities observed for oceanic P propagating near to the trend of the array (Japanese and Kuril data) are consistent with compressional wave anisotropy observed in refraction experiments. The observation that oceanic S also has an apparent minimum velocity near the strike of magnetic lineations is an interesting and additional constraint on the symmetry form of the material anisotropy.

In the locale north of the OBH line array, the magnetic lineations trend NW–SE. In the area of and south of the array the trends are not distinguished in the magnetic quiet zone. For oceanic P and S propagation paths from Japan and the Kurils the strike of magnetic lineations changes dramatically across the Shatsky Rise. The NW Pacific basin between the Shatsky Rise and Japan is characterized by SW–NE trending lineations. In propagating from Japan and the Kurils to the OBH array, the oceanic P and S are first perpendicular (more or less) to the local magnetic lineations, then past the Shatsky Rise the paths are nearly parallel to the lineations. Thus, assuming a material anisotropy with the slow direction in the direction of the lineaments and the fast direction perpendicular to the lineaments, then the oceanic P and S would be travelling faster west of the Shatsky Rise than in the area of the OBH line array SE of the Shatsky Rise.

The data from events in the Kurils and northern Honshu have propagation paths across the Shatsky Rise, at which Den *et al.* (1969) observed Moho velocities in the range of 8.2. From the Izu–Bonin Islands the propagation paths of oceanic P and S from events 8 and 9 in Fig. 1 to the OBH line array cross only ocean basin. The azimuth of propagation at the array is 16° counter-clockwise from the local magnetic lineations. About 55 per cent of the path parallels magnetics at this shallow angle. South-west of the Shatsky Rise the magnetic lineations rotate direction, and the remaining 45 per cent of the propagation path crosses magnetics at about a 60° angle. If the apparent velocity, $7.9\,\mathrm{km\,s^{-1}}$, is assumed for 55 per cent of the path with a strike near the lineaments, a velocity of $8.48\,\mathrm{km\,s^{-1}}$ may be derived for the 45 per cent of the propagation path at a steep angle to the magnetics if the time intercept is set to zero. This is a reasonable first approximation for the intercept time in the absence of a good model of the P waveguide – for positive time intercepts, even higher velocities are derived.

In the north-western Pacific where the P and S velocities are predicted to be faster, Shimamura & Asada (1983) and Shimamura (1984) detected compressional velocity anisotropy with the maximum velocity perpendicular to the magnetic lineations. In the distance range 140–1800 km the azimuthal velocity variation may be fit with $V = 8.15 \pm 0.55\,\mathrm{km\,s^{-1}}$ and a $\cos 2\theta$ symmetry. Shimamura & Asada (1983) and Shimamura (1984) claim direct evidence that the anisotropy extends to deeper portions of the lithosphere in the observed offsets in travel-time curves, implying a mid-lithosphere low-velocity zone (Shimamura & Asada 1976; Shimamura, Asada & Kumazawa 1977).

The P and S phases discussed in this study are high-frequency (2–15 Hz) phases travelling great distances with velocities appropriate for Pn and Sn. The high-frequency content implies a high Q propagation path within the lithosphere. Propagation through only a part of a low Q asthenosphere would rapidly attenuate these phases. The propagation mode within the lithosphere is still uncertain, but a low-velocity zone within the lithosphere may act as a waveguide (Nagumo *et al.* 1981; Butler 1983). Mid-lithosphere low-velocity zones characterized by 4.2–10.6 per cent velocity decreases within the Pacific lithosphere have been inferred in the P-wave data of Shimamura & Asada (1976), Orcutt & Dorman (1977) and Nagumo *et al.* (1981). The observations presented here, together with results of Shimamura & Asada (1983) and Shimamura (1984) in the NW Pacific basin, suggest that a large part or all of the western Pacific lithosphere is azimuthally anisotropic for both P- and S-waves.

The corresponding lack of evidence for azimuthal anisotropy in the long-period surface wave data becomes interesting at this stage. Surface wave studies (e.g. Schlue & Knopoff 1976; Yu & Mitchell 1979) in the Pacific have determined that the azimuthal anisotropy cannot be greater than 0.8 per cent. In the westernmost Pacific where the regional fabric of magnetic lineations shows great variability on either side of the Shatsky Rise, the surface wave data would be an average over these variations, and therefore the lack of evidence for azimuthal anisotropy in this instance is not unexpected. In the central and eastern Pacific, however, very large regions have a similar fabric of magnetic lineations. In these younger regions of the Pacific we cannot necessarily extrapolate our result of a largely anisotropic lithosphere as found in the old western Pacific. Without some mechanism for the degree of anisotropy to increase with age, it seems logical to assume that the younger central and eastern Pacific lithosphere is also anisotropic. One possible mechanism, however, is lithosphere drag (Ave'Lallemant & Carter 1970), which has been discussed by Kirkwood & Crampin (1981). The only direct evidence for azimuthal anisotropy is in the uppermost, sub-Moho lithosphere from the seismic refraction data discussed earlier (e.g. Morris *et al.* 1969; Bibee & Shor 1976). Surface wave studies (e.g. Mitchell & Yu 1980) have broad resolving kernels (~ 40–400+ depth) and therefore average over fine structure. Before the anisotropic results presented here and by Shimamura & Asada (1983) and Shimamura (1984) it had been argued (e.g. Francis 1969; Whitmarsh 1971) that the azimuthal anisotropy observed in the marine seismic refraction data represented a thin veneer at the base of the Moho, and as such was not substantially sampled by the long-period surface wave data. For the western Pacific at least, the results presented here show that restricting anisotropy to a thin veneer is incapable of explaining the data.

Conclusions

Several conclusions may be drawn from the Walker & McCreery (1985) data set obtained in the Wake OBH line array experiment.

(1) Average apparent velocities measured for *P*- and *S*-waves by the array are slower than average group velocities for propagation paths from Japan and the Kurils.

(2) When the apparent velocity data are organized azimuthally, a pattern can be seen wherein propagation paths at shallow angles to the array and the local magnetic lineations exhibit slower apparent velocities than paths at steep angles.

(3) The azimuthal velocity variation may be consistent with azimuthal anisotropy. As the *P* and *S* data propagate to distances of 20° to $37^\circ\Delta$ within the lithosphere, this also implies that a large part of the western Pacific lithosphere is likely to be anisotropic.

(4) The *Pn* and *Sn* velocities of 8.3 and 4.8 km s^{-1}, respectively, observed in the NW Pacific by Walker & Sutton (1971), Sutton & Walker (1972) and Walker (1977) represent average velocities over provinces within the north-western Pacific basin characterized by a range of seismic velocities. With azimuthal anisotropy the local apparent velocity of oceanic *P* and *S* depends upon the azimuth of propagation.

(5) Observed slow velocities of oceanic *P* and *S* have propagation paths with azimuths at shallow angles to nearby magnetic lineations, and faster data arrive at steeper angles. This velocity variation is noted in the compression wave marine refraction studies (e.g. Raitt *et al.* 1969; Morris *et al.* 1969). If velocity as a function of strike from the magnetic lineations is presumed, then the diversity of directions of magnetic lineations in the north-western Pacific (particularly on either side of the Shatsky Rise) implies a laterally heterogenerous velocity distribution along paths of oceanic *P* and *S* that propagate great distances in the lithosphere of the western Pacific.

(6) This is the first observation of an anisotropic character of *S*-wave propagation in the

oceanic lithosphere. Since the data are recorded on hydrophones, the polarization of S is SV to be coupled to the water. Velocities of oceanic S observed in the >150 Ma western Pacific (for propagation nearly parallel to the local magnetic lineations) are comparable to the 4.58 km s^{-1} value that Hart & Press (1973) found for *Sn* in the <50 Ma regionalized Atlantic.

Acknowledgments

I thank Dan Walker and Chip McCreery for making their data available to me in advance of publication. I thank Dan Walker and Gerard Fryer for reviewing this manuscript. This research was supported by the Office of Naval Research. Hawaii Institute of Geophysics Contribution No. 1562.

References

Anderson, D. L., 1966. Recent evidence concerning the structure and composition of the Earth's mantle, *Phys. Chem. Earth*, **6**, 1–131.

Anderson, D. L. & Regan, J., 1983. Upper mantle anisotropy and the oceanic lithosphere, *Geophys. Res. Lett.*, **10**, 9, 841–844.

Ave'Lallemant, H. G. & Carter, N. L., 1970. Syntectonic recrystallization of olivine and modes of flow in the upper mantle, *Bull. geol. Soc. Am.*, **81**, 2203–2220.

Backus, G. E., 1965. Possible forms of seismic anisotropy of the upper mantle under oceans, *J. geophys. Res.*, **70**, 3429–3439.

Bibee, L. D. & Shor, G. G., 1976. Compressional wave anisotropy in the crust and upper mantle, *Geophys. Res. Lett.*, **3**, 639–642.

Butler, R., 1983. Seismic studies of the Shatsky Rise and Ontong Java Plateau, *Eos Trans.*, **64**, 939.

Den, N., Ludwig, W. J., Murauchi, S., Ewing, J. I., Hotta, H., Edgar, N. T., Yoshi, T., Asanuma, T., Hagiwara, K., Sato, T. & Ando, S., 1969. Seismic-refraction measurements in the northwest Pacific basin, *J. geophys. Res.*, **74**, 1421–1434.

Forsyth, D. W., 1975a. The early structural evolution and anisotropy of the oceanic upper mantle, *Geophys. J. R. astr. Soc.*, **43**, 103–162.

Forsyth, D. W., 1975b. A new method for the analysis of multi-mode surface wave dispersion: application to Love wave propagation in the east Pacific, *Bull. seism. Soc. Am.*, **65**, 323–342.

Francis, T. J. G., 1969. Generation of seismic anisotropy in the upper mantle along the mid-ocean ridges, *Nature*, **221**, 162–165.

Hart, R. S. & Press, F., 1973. *Sn* velocities and the composition of the lithosphere in the regionalized Atlantic, *J. geophys. Res.*, **78**, 407–411.

Hess, H., 1964. Seismic anisotropy of the uppermost mantle under oceans, *Nature*, **203**, 629.

Hilde, T. W. C., Isezaki, N. & Wageman, J. M., 1976. Mesozoic sea-floor spreading in the North Pacific, in *The Geophysics of the Pacific Ocean Basin and its Margins*, eds Sutton, G. H., Manghnani, M. H. & Moberly, R., *Geophys. Monogr. Ser. Am. geophys. Un.*, **19**, pp. 205–226, American Geophysical Union, Washington, DC.

Keen, C. E. & Barrett, D. L., 1971. A measurement of seismic anisotropy in the northeast Pacific, *Can. J. Earth Sci.*, **8**, 1056–1065.

Kirkwood, S. C. & Crampin, S., 1981. Surface-wave propagation in an ocean basin with an anisotropic upper mantle: observations of polarization anomalies, *Geophys. J. R. astr. Soc.*, **64**, 487–497.

Knopoff, L., 1983. The thickness of the lithosphere from the dispersion of surface waves, *Geophys. J. R. astr. Soc.*, **74**, 55–81.

Larson, R. L., 1976. Late Jurassic and early Createaceous evolution of the western central Pacific Ocean, *J. Geomagn. Geoelect.*, **28**, 219–236.

McCreery, C. S. & Sutton, G. H., 1980. Wave train characteristics of long-range, high-frequency *Pn, Sn* crossing an ocean bottom hydrophone array, *Bull. seism. Soc. Am.*, **70**, 437–446.

McEvilly, T. V., 1964. Central U.S. crust-upper mantle structure from Love and Rayleigh wave phase velocity inversion, *Bull. seism. Soc. Am.*, **54**, 1997–2016.

Mitchell, B. J. & Yu, G.-K., 1980. Surface wave dispersion, regionalized velocity models, and anisotropy of the Pacific crust and upper mantle, *Geophys. J. R. astr. Soc.*, **63**, 497–514.

Morris, G. B., Raitt, R. W. & Shor, G. G., 1969. Velocity anisotropy and delay-time maps of the mantle near Hawaii, *J. geophys. Res.*, **74**, 4300–4316.

Nagumo S., Ouchi, T., Kasahara, J., Koresawa, S., Tomoda, Y., Kobayashi, K., Furumoto, A. S., Odegard, M. E. & Sutton, G. H., 1981. Sub-moho seismic profile in the Mariana basin – ocean bottom seismograph long-range explosion experiment *Earth planet. Sci. Lett.*, **53**, 93–102.

Orcutt, J. A. & Dorman, L. M., 1977. An oceanic long range explosion experiment: a preliminary report, *J. geophys.*, **43**, 257–263.

Raitt, R. W., 1969. Anisotropy of the upper mantle, in *The Earth's Crust and Upper Mantle*, ed. Hart, P. J., *Geophys. Monogr. Ser. Am. geophys. Un.*, **13**, pp. 250–256, American Geophysical Union, Washington, DC.

Raitt, R. W., Shor, G. G., Francis, T. J. G. & Morris, G. B., 1969. Anisotropy of the Pacific upper mantle, *J. geophys. Res.*, **74**, 3095–3109.

Raitt, R. W., Shor, G. G., Morris, G. B. & Kirk, H. K., 1971. Mantle anisotropy in the Pacific Ocean, *Tectonophys.*, **12**, 173–186.

Schlue, J. W. & Knopoff, L., 1976. Shear wave anisotropy in the upper mantle of the Pacific Basin, *Geophys. Res. Lett.*, **3**, 359–362.

Schlue, J. W. & Knopoff, L., 1977. Shear wave polarization anisotropy in the Pacific basin, *Geophys. J. R. astr. Soc.*, **49**, 145–165.

Schlue, J. W. & Knopoff, L., 1978. Inversion of surface-wave phase velocities for an anisotropic structure, *Geophys. J. R. astr. Soc.*, **54**, 697–702.

Shimamura, H., 1984. Anisotropy in the oceanic lithosphere of the Northwestern Pacific basin, *Geophys. J. R. astr. Soc.*, **76**, 253–260.

Shimamura, H. & Asada, T., 1976. Apparent velocity measurements on an oceanic lithosphere, *Phys. Earth planet. Int.*, **13**, 15–22.

Shimamura, H. & Asada, T., 1983. Velocity anisotropy extending over the entire depth of the oceanic lithosphere, in *Final Report of the International Geodynamics Program*, pp. 121–125, Geodynamics Series (Working Group 1), ed. Hilde, T. W. C., American Geophysical Union, Washington, DC.

Shimamura, H., Asada, T. & Kumzawa, M., 1977. High shear velocity layer in the upper mantle of the Western Pacific, *Nature*, **269**, 680–682.

Smith, M. L. & Dahlen, F. A., 1973. The azimuthal dependence of Love and Rayleigh wave propagation in a slightly anisotropic medium, *J. geophys. Res.*, **78**, 17, 3321–3333.

Snedecor, G. W. & Cochran, W. G., 1967. *Statistical Methods*, Iowa State University Press, Ames Iowa.

Sutton, G. H., McCreery, C. S., Duennebier, F. K. & Walker, D. A., 1978. Spectral analysis of high-frequency *Pn*, *Sn* phases recorded on ocean bottom seismographs, *Geophys. Res. Lett.*, **5**, 745–747.

Sutton, G. H. & Walker, D. A., 1972. Oceanic mantle phases recorded on seismograms in the northwestern Pacific at distances between 7° and 40°, *Bull. seism. Soc. Am.*, 42, 631–645.

Talandier, J. & Bouchon, M., 1979. Propagation of high frequency *Pn* waves at great distances in the central and south Pacific and its implications for the structure of the lower lithosphere, *J. geophys. Res.*, **84**, 5613–5619.

Walker, D. A., 1977. High frequency *Pn* phases observed in the Pacific at great distances, *Science*, **197**, 257–259.

Walker, D., 1982. Oceanic *Pn/Sn* phases: a qualitative explanation and reinterpretation of the *T*-phase, *Hawaii Inst. Geophys. Rept HIG-82-6*, 19 pp.

Walker, D. A. & McCreery, C. S., 1985. *Po/So* phases: propagation velocity and attenuation across a 1600 km long deep ocean hydrophone array, *J. geophys. Res.*, submitted.

Walker, D. A., McCreery, C. S. & Sutton, G. H., 1983. Spectral characteristics of high-frequency *Pn, Sn* phases in the western Pacific, *J. geophys. Res.*, **88**, 4289–4298.

Walker, D. A., McCreery, C. S., Sutton, G. H. & Duennebier, F. K., 1978. Spectral analysis of high-frequency *Pn* and *Sn* phases observed at great distance in the western Pacific, *Science*, **199**, 1333–1335.

Walker, D. A. & Sutton, G. H., 1971. Oceanic mantle phases recorded on hydrophones in the northwestern Pacific at distances between 9° and 40°, *Bull. seism. Soc. Am.*, **61**, 65–78.

Whitmarsh, R. B., 1971. Seismic anisotropy of the uppermost mantle absent beneath the east flank of the Reykjanes Ridge, *Bull. seism. Soc. Am.*, **61**, 1351–1386.

Yu, G.-K. & Mitchell, B. J., 1979. Regionalized shear velocity models of the Pacific upper mantle from observed Love and Rayleigh wave dispersion, *Geophys. J. R. astr. Soc.*, **57**, 311–341.